Korean J. of Chem. Eng., **10**(4), 226-234 (1993)

DISSIPATIVE STRUCTURES OF AUTOCATALYTIC REACTIONS IN TUBULAR FLOW REACTORS

Sang Hwan Kim* and Hyung-Sang Park

*Department of Chemical Engineering, Konkuk University, Seoul 133-701, Korea
Department of Chemical Engineering, Sogang University, Seoul 121-742, Korea
(Received 13 May 1993 • accepted 16 August 1993)

Abstract—Dissipative structures of autocatalytic reactions with initially uniform concentrations are studied in tubular flow reactors. A unique steady state exists in a continuous stirred tank reactor. Linear stability analysis predicts either a stable node, a focus or an unstable saddle-focus. Sustained oscillations around the unstable focus can occur for high values of Damköhler number. In distributed parameter systems, travelling, standing or complex oscillatory waves are detected. For low values of Damköhler number, travelling waves with pseudo-constant patterns are observed. With intermediate values of Damköhler number, single or multiple standing waves are obtained. The temporal behavior indicates also the appearance of retriggering or echo waves. For high values of Damköhler number, both single peak and complex multipeak oscillations are found. In the cell model, both regular oscillations near the inlet and chaotic behavior downstream are observed. In the dispersion model, higher Peclet numbers eliminate the oscillations. The spatial profile shows a train of pulsating waves for the discret model and a single pulsating or solitary wave for the continuous model.

INTRODUCTION

Autocatalytic reactions represent a very important class of chemical reactions with a variety of applications in combustion, biological reactors, and homogeneous and catalytic reactors. To mention only a few: Lotka's model on population dynamics [1], the Brusselator description of theoretical tri-molecular reactions [2-5], the Belousov-Zhabotinskii reaction [6-7], the modified Lotka-Volterra model for hydrocarbon oxidation and cool flames [8], and Yamazaki's reaction [9].

There are striking parallels between isothermal autocatalytic and exothermic first-order reactions. While there is a systematic analysis available on exothermic reaction systems, no extensive study has been made of the corresponding isothermal autocatalytic prototypes where the feedback is not thermal but autocatalytic. Fascinating dissipative structures (spatially, temporally or even spatiotemporally organized states) have been studied both theoretically and experimentally [2-7]. Among them, symmetry breaking structures, wave trains including planar and standing waves, and target, spiral and scroll patterns as well as chaotic behavior have drawn the attention of mathematicians, physicists, biologists, chemists and chemical engineers.

The Belousov-Zhabotinskii reaction, oxidation of malonic acid by potassium bromate with ceric/cerous ions as catalysts, has been extensively studied. Tatterson and Hudson [10] observed chemical waves of pulse type propagating in a tube, in the absence of convection effects. Frequency, speed and wavelength did not change significantly during the process. This observation reveals the rich spectrum of wave phenomena in the Belousov-Zhabotinskii reaction [11]. Marek and Svobodová [12] observed experimentally sustained oscillations and jump phenomena (transition of oscillatory behavior to steady states) in a continuous stirred tank reactor (CSTR) and standing as well as travelling waves in tubular flow reactors. Schmitz, Hudson and Graziani [13-14] established simple singlepeak and complex multipeak oscillations, and chaotic behavior in a CSTR. Rössler [15] also observed an irregular screw-type chaotic behavior in a CSTR. Simoyi et al. [16] noticed subharmonic bifurcations of a limit cycle leading to alternating complex periodic and chaotic regimes in a CSTR. Roux [17] studied experimentally bifurcations of a limit cycle leading to quasi-periodic oscillations.

To our knowledge, no systematic studies have been

*Author to whom correspondence should be addressed.

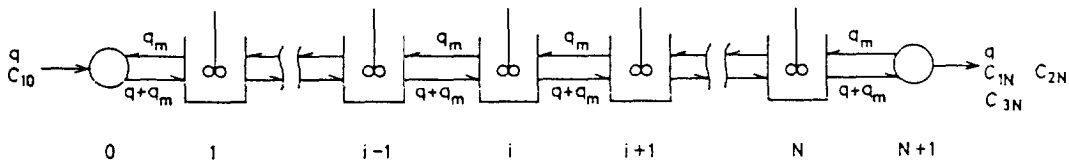

Fig. 1. Schematic sketch of the cell model with backflow, q_m.

reported on dissipative structures of autocatalytic reactions occurring in distributed parameter flow systems, for example, tubular flow reactors. In this paper we attempt to comprehend the interplay of transport processes, such as diffusion, convection and complex autocatalytic kinetics. One-dimensional (1D) model is considered. Emphasis is placed on the problems of local stability in a CSTR, wave propagation phenomena for standing, travelling and spatio-temporal waves, and chaotic behavior. Possible differences between discrete and continuous descriptions of distributed parameter flow systems will be discussed.

GOVERNING EQUATIONS

Consider the following reactions whose rates are described by Eq. (1). These autocatalytic reactions give rise to undamped oscillations in a closed system [18].

$$R_1=\frac{dC_1}{dt}=k_1C_1-k_3C_1C_3$$

$$R_2=\frac{dC_2}{dt}=k_1C_1-k_2C_2$$

$$R_3=\frac{dC_3}{dt}=k_2C_2-k_3C_3 \tag{1}$$

In this paper we are analyzing an isothermal autocatalytic system occurring in tubular flow reactors.

Two distinct types of description of mass dispersion in tubular flow reactors have been adopted so far. The dispersion model assumes that the transport may be phrased in terms of continuous description while the cell model visualizes the behavior of tubular flow reactors by a sequence of well-stirred tank reactors as shown in Fig. 1. It has been shown in the literature [19-20] that certain differences, particularly concerning multiplicity, do exist between cell and dispersion models for an exothermic first-order reaction. Therefore, both the cell model with backflow and the dispersion model are considered. Isothermal conditions, an identical volume of each cell, same back-flow rates for all components, and no changes of physical properties are assumed in the present paper.

Mass balances around the i-th tank in the one-dimensional cell model as shown in Fig. 1, yield the following dimensionless differential-difference equations [28]:

$$\begin{aligned}\frac{dU_i}{d\tau}&=(1+K_m)U_{i-1}-(1+2K_m)U_i+K_mU_{i+1}\\&\quad+Da(U_i-\alpha_1U_iW_i)\\\frac{dV_i}{d\tau}&=(1+K_m)V_{i-1}-(1+2K_m)V_i+K_mV_{i+1}\\&\quad+Da(U_i-\alpha_2V_i)\\\frac{dW_i}{d\tau}&=(1+K_m)W_{i-1}-(1+2K_m)W_i+K_mW_{i+1}\\&\quad+Da(\alpha_2V_i-\alpha_3W_i).\end{aligned} \tag{2}$$

The mass balance of two fictitious cells, 0 and N+1, gives

$$\begin{aligned}&i=0: &&(1+K_m)U_0=1+K_mU_1\\&&&(1+K_m)V_0=K_mV_1\\&&&(1+K_m)W_0=K_mW_1\\&i=N+1: &&U_{N+1}=U_N\ V_{N+1}=V_N\ W_{N+1}=W_N.\end{aligned} \tag{3}$$

The corresponding dispersion model is described by three coupled partial differential equations of parabolic type [28]:

$$\begin{aligned}\frac{\partial U}{\partial\tau}&=\frac{1}{Pe}\frac{\partial^2U}{\partial x^2}-\frac{\partial U}{\partial x}+Da(U-\alpha_1UW)\\\frac{\partial V}{\partial\tau}&=\frac{1}{Pe}\frac{\partial^2V}{\partial x^2}-\frac{\partial V}{\partial x}+Da(U-\alpha_2V)\\\frac{\partial w}{\partial\tau}&=\frac{1}{Pe}\frac{\partial^2W}{\partial x^2}-\frac{\partial W}{\partial x}+Da(\alpha_2V-\alpha_3W)\end{aligned} \tag{4}$$

subject to Danckwerts boundary conditions

$$\begin{aligned}&x=0,\ \tau>0: &&1=U-\frac{1}{Pe}\frac{\partial U}{\partial x}\\&&&V=\frac{1}{Pe}\frac{\partial V}{\partial x}\\&&&W=\frac{1}{Pe}\frac{\partial W}{\partial x}\\&x=N,\ \tau>0: &&\frac{\partial U}{\partial x}=\frac{\partial V}{\partial x}=\frac{\partial W}{\partial x}=0.\end{aligned} \tag{5}$$

Here we have denoted by U, V, W the dimensionless concentrations of C_1, C_2 and C_3, respectively. α_1, α_2,

and α_3 are dimensionless kinetic constants. Da is the Damköhler number, K_m the mass backflow ratio, Pe axial particle Peclet number for mass, and τ the dimensionless time defined by

$$U_i=\frac{C_{1i}}{C_{10}} \quad V_i=\frac{C_{2i}}{C_{10}} \quad W_i=\frac{C_{3i}}{C_{10}}$$

$$Da=\frac{v}{q}k_1 \quad K_m=\frac{q_m}{q} \quad Pe=\frac{ud_p}{D} \quad \tau=\frac{qt}{v}$$

$$\alpha_1=\frac{C_{10}k_3}{k_1} \quad \alpha_2=\frac{k_2}{k_1} \quad \alpha_3=\frac{k_3}{k_1} \quad x=\frac{z}{d_p}. \tag{6}$$

ANALYSIS AND NUMERICAL RESULTS

Numerical integration of sets of ordinary differential Eqs. (2)-(3) was performed using Gear's method for integration of stiff systems of ordinary differential equations. The error of integration was controlled to six decimal places. The set of nonlinear parabolic partial differential Eqs. (4)-(5) was integrated by a Crank-Nicolson method with an automatic time-step adjustment. The error of integration was controlled to four significant decimal places. The majority of calculations was performed using forty mixing cells (N=40) in the axial direction. In order to compare the results from both models, the dimensionless length(x) in the dispersion model was converted into the equivalent number of cells(i) in the corresponding cell model.

1. Lumped parameter systems

A detailed understanding of lumped parameter systems may provide a deeper insight into the dynamics of corresponding distributed parameter systems. For a single CSTR, Eq. (2) is simplified to a three variable system represented by Eq. (7):

$$\frac{dU}{d\tau}=1-U+Da(U-\alpha_1UW)=F(U, V, W)$$

$$\frac{dV}{d\tau}=-V+Da(U-\alpha_2V)=G(U, V, W)$$

$$\frac{dW}{d\tau}=-W+Da(\alpha_2V-\alpha_3W)=H(U, V, W). \tag{7}$$

The presence of multiple steady states in Eq. (7) can be evaluated by setting F, G, and H equal to zero and analyzing the resulting set of three nonlinear algebraic equations. Among the four governing parameters in Eq. (7), the Damköhler number (Da) is the most important parameter for understanding the properties of flow systems. After simple algebraic manipulations a quadratic equation results for the concentration U_s (the subscript s refers to steady state conditions):

$$\alpha U_s^2+\beta U_s+\gamma=0. \tag{8}$$

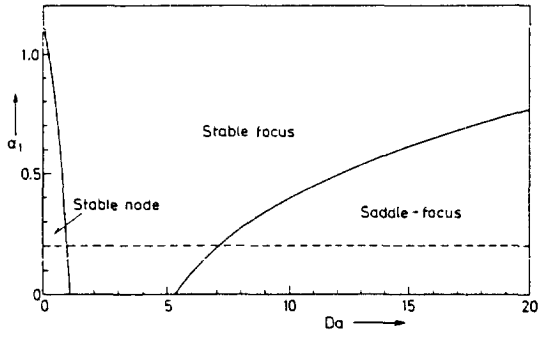

Fig. 2. Local stability region in the CSTR.
$\alpha_2=\alpha_3=0.2$.

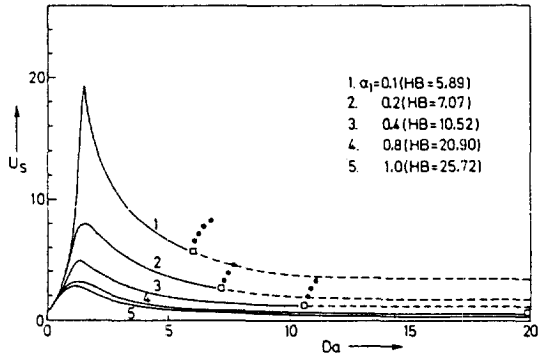

Fig. 3. Steady states versus Damköhler number in the CSTR.
$\alpha_2=\alpha_3=0.2$ (□ and HB denote Hopf-bifurcation points). — stable steady state; ····· unstable steady state; ●●●● stable periodic solution.

Constants α, β, and γ are defined by

$$\alpha=\alpha_1\alpha_2 \ Da^3$$
$$\beta=1+(\alpha_2+\alpha_3-1)Da-\alpha_3Da^2-\alpha_2\alpha_3Da^3$$
$$\gamma=-1-(\alpha_2+\alpha_3)Da-\alpha_2\alpha_3Da^2. \tag{9}$$

Although multiple steady states are frequently observed in autocatalytic systems, our analysis revealed that for the autocatalytic system in question, multiple solutions do not exist.

Local stability properties in a region close to steady states can be predicted from the eigenvalues, λ, satisfying the cubic equation

$$\lambda^3+\delta\lambda^2+\varepsilon\lambda+\zeta=0. \tag{10}$$

Here the constants δ, ε, and ζ can be obtained as follow:

$$\delta=-\left(\frac{\partial F}{\partial U}\right)_s-\left(\frac{\partial G}{\partial V}\right)_s-\left(\frac{\partial H}{\partial W}\right)_s$$

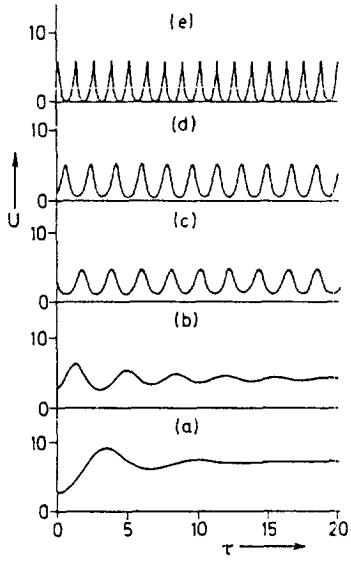

Fig. 4. Time evolution depending on the Damköhler number in the CSTR.
$\alpha_1=\alpha_2=\alpha_3=0.2$. Da is: (a) 2.0, (b) 4.0, (c) 8.0, (d) 10.0, (e) 16.0.

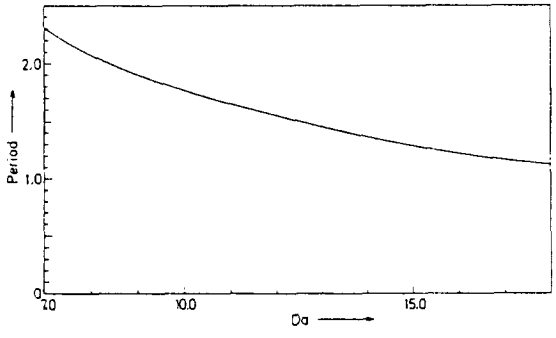

Fig. 5. Period of oscillations versus Damköhler number in the CSTR.
$\alpha_1=\alpha_2=\alpha_3=0.2$.

$$\varepsilon=\left(\frac{\partial F}{\partial U}\right)_s\left(\frac{\partial G}{\partial V}\right)_s+\left(\frac{\partial F}{\partial U}\right)_s\left(\frac{\partial H}{\partial W}\right)+\left(\frac{\partial G}{\partial V}\right)_s\left(\frac{\partial H}{\partial W}\right)_s$$

$$\zeta=-\left(\frac{\partial F}{\partial U}\right)_s\left(\frac{\partial G}{\partial V}\right)_s\left(\frac{\partial H}{\partial W}\right)_s-\left(\frac{\partial F}{\partial W}\right)_s\left(\frac{\partial G}{\partial U}\right)_s\left(\frac{\partial H}{\partial V}\right)_s \quad (11)$$

Linear stability analysis shows that a stable node and a focus, and an unstable saddle-focus may exist in the CSTR as shown in Fig. 2. A stable limit cycle may occur around unstable steady states (see Fig. 3). Hopf-bifurcation points occur at high values of Da with increasing values of kinetic constants α_1 as depicted

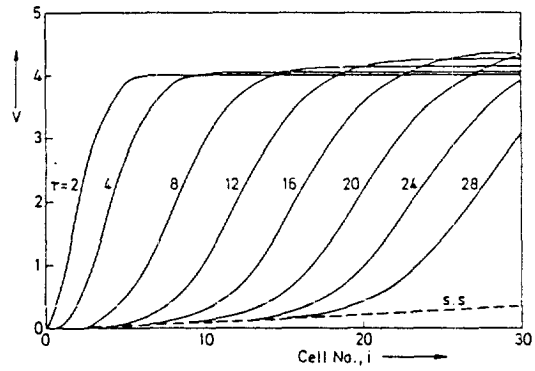

Fig. 6. Travelling waves in a tubular system.
Da=0.01, $\alpha_1=\alpha_2=\alpha_3=0.2$ (s.s. denotes steady states).

in Fig. 3. The oscillatory behavior exists in the region of higher Da's, i.e., at low flow rates with higher feed concentrations. Low flow rates favor the oscillations while higher flow rates result in steady state modes of operation (see Fig. 4). These trends are in accordance with experimental observations on the Belousov-Zhabotinskii reaction taking place in a CSTR [13-16]. Isolas and mushrooms in steady state diagrams "concentration versus flow rates", which Gray observed for his quadratic and cubic autocatalytic reactions [21], are not detected in our system.

The period of oscillations increases with decreasing values of Da, see Fig. 5. This result is in qualitative agreement with experimental observations obtained by Marek [12] on the Belousov-Zhabotinskii reaction in a CSTR.

2. Distributed parameter systems

Wave phenomena in distributed parameter systems can be qualitatively explained as a kind of interaction between two or more coupled or forced oscillators. Pismen [22] analyzed conditions for spatial and/or temporal order to emerge from a homogeneous steady state: such as inhomogeneous oscillating states (wave patterns). Neu [23], using singular pertubation analysis around homogeneous oscillatory states, studied in detail the phase desynchronization of two coupled oscillators in order to develop criteria for wave propagation.

Apart from phase desynchonization, external gradients and inhomogeneities, the geometry of systems, and initial conditions can also play an important role in wave propagation phenomena (target, spiral waves and scroll patterns).

The analysis presented below considers only one component, C_1, in the feed ($C_2=C_3=0$). Initial condi-

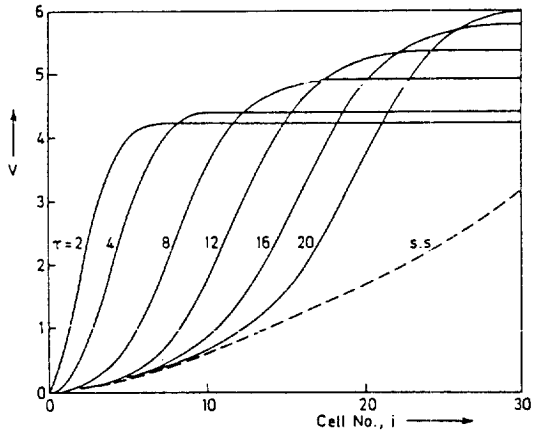

Fig. 7. Travelling waves in a tubular system.
Da=0.05, $\alpha_1=\alpha_2=\alpha_3=0.2$.

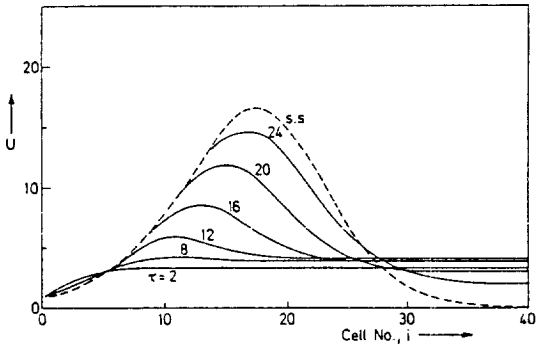

Fig. 8. Single standing wave in a tubular system.
Da=0.20, $\alpha_1=\alpha_2=\alpha_3=0.2$.

tions considered are U=3.0, V=W=4.0.

As shown in Figs. 6-11, travelling waves are observed at low Da's while standing waves prevail at intermediate values of Da. The Damköhler number can be expressed as the ratio of the characteristic time for bulk mass flow to that for chemical reactions. Therefore, high flow rates favor travelling wave phenomena while intermediate flow rates support the occurrence of standing waves.

The velocity of travelling waves increases slightly during the initial stage, passes through the maximum, and then decreases again before approaching particular stable structures in space. The shape of travelling waves depicted in Figs. 6-7 is continually changing. This trend is typical for problems featuring high values of Da.

Steady state profiles presented in Figs. 6-11 show the typical features of spatial structures. Increasing values of Da modifies wave patterns from a travelling

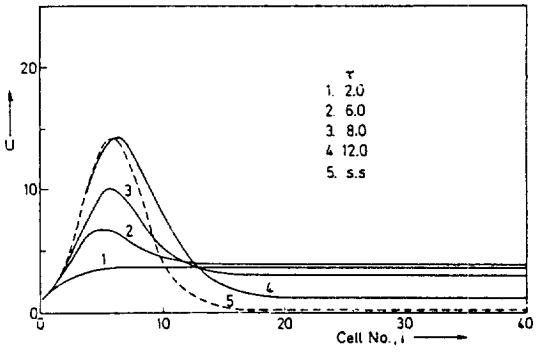

Fig. 9. Single standing wave in a tubular system.
Da=0.50, $\alpha_1=\alpha_2=\alpha_3=0.2$.

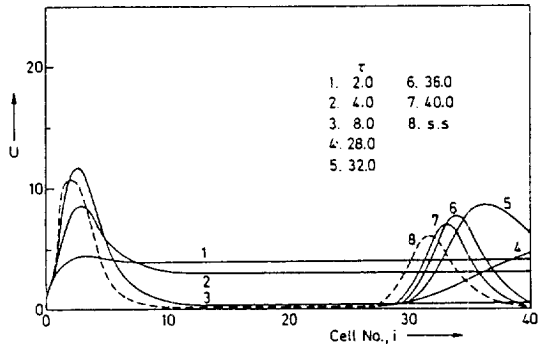

Fig. 10. Multiple standing waves in a tubular system.
Da=1.00, $\alpha_1=\alpha_2=\alpha_3=0.2$.

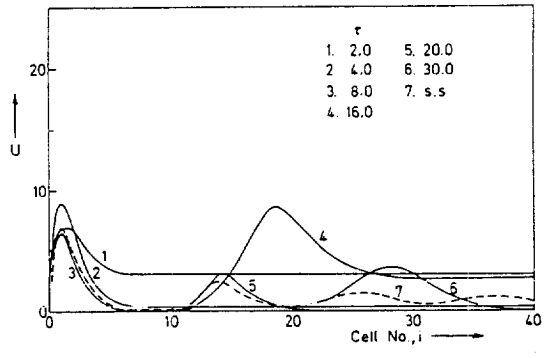

Fig. 11. Multiple standing waves in a tubular system.
Da=2.00, $\alpha_1=\alpha_2=\alpha_3=0.2$.

to a standing wave. The transition occurs around Da≅ 0.1. Standing waves in Figs. 10-11 remind one of the characteristics of triggering waves emerging from a uniform homogeneous state. A single spatial structure (or standing wave) appears in Figs. 8-9 in the region near the inlet.

With increasing values of Da, Figs. 10-11, two or

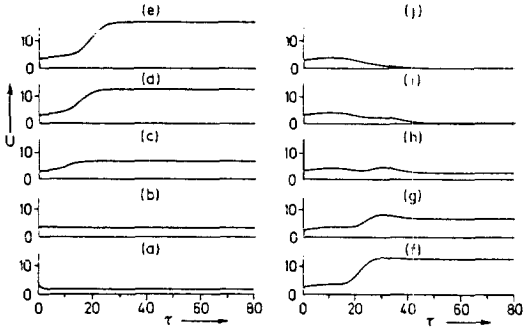

Fig. 12. Temporal behavior at different positions in a tubular system.
Da=0.20, $\alpha_1=\alpha_2=\alpha_3=0.2$. Cell No. is: (a) 1, (b) 5, (c) 9, (d) 13, (e) 17, (f) 21, (g) 25, (h) 29, (i) 33, (j) 37.

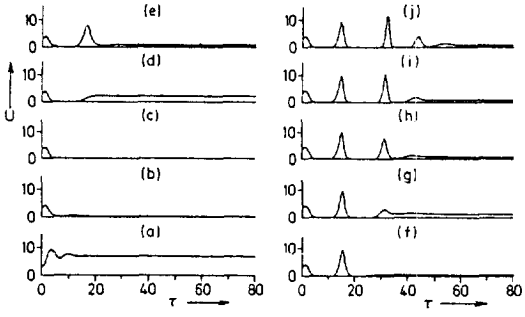

Fig. 13. Temporal behavior at different positions in a tubular system.
Da=2.0, $\alpha_1=\alpha_2=\alpha_3=0.2$. Cell No. is: (a) 1, (b) 5, (c) 9, (d) 13, (e) 17, (f) 21, (g) 25, (h) 29, (i) 33, (j) 37.

more triggering waves or multiple standing waves appear in the system, after the first standing wave has already developed upstream near the inlet. This phenomenon may be elucidated in terms of a retriggering process or echo wave, originally proposed by Krinsky [24] for two coupled monostable generators. Consider two coupled elements at rest. Then, if one element is excited, the second also becomes excited after some delay Δ. If the delay time (Δ) happens to lie between the refractory and the excitement time (i.e., $T_R<\Delta<T_E$), a retriggering wave may propagate in distributed systems. The time history for travelling and standing waves at different positions in the flow system is shown in Figs. 12 and 13, respectively. Fig. 13 reminds one of the behavior of retriggering waves. The dynamical behavior of the cell model thus turns out to be in good qualitative agreement with that in the corresponding dispersion model. In the range of low Da's leading to a stable state, the backflow for mass has no qualitative effect on the dynamics of autocalytic reactions.

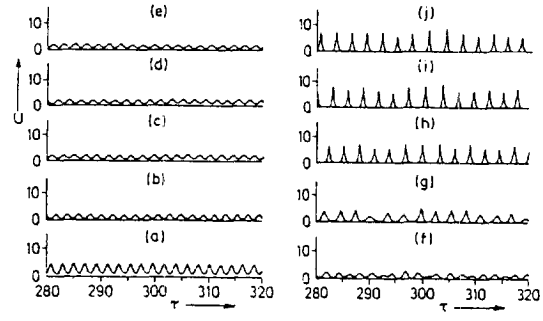

Fig. 14. Comparison of the oscillations at different positions in the 1-D cell model.
Da=8.0, $\alpha_1=\alpha_2=\alpha_3=0.2$. $K_m=0.0$. Cell No. is: (a) 1, (b) 5, (c) 9, (d) 13, (e) 17, (f) 21, (g) 25, (h) 29, (i) 33, (j) 37.

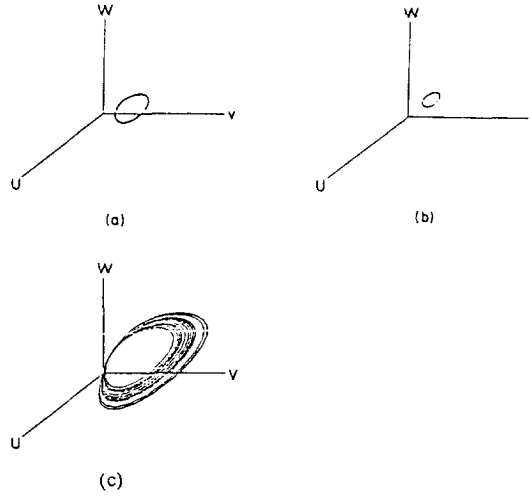

Fig. 15. Three-dimensional stereoplot at different positions in the 1-D cell model.
Da=8.0, $\alpha_1=\alpha_2=\alpha_3=0.2$. $K_m=0.0$. Cell number is: (a) 1, (b) 9, (c) 33.

Based on the analysis for a single CSTR we can expect complex oscillatory behavior for high values of Da. Temporal behavior of concentrations at different positions in the tubular system, calculated from the 1-D cell model with no backflow ($K_m=0.0$) is shown in Fig. 14. The oscillatory profile of limit cycle type, generated in the first cell, propagates downstream the system. The amplitude of the "limit cycle" shrinks and the regular behavior changes toward com-

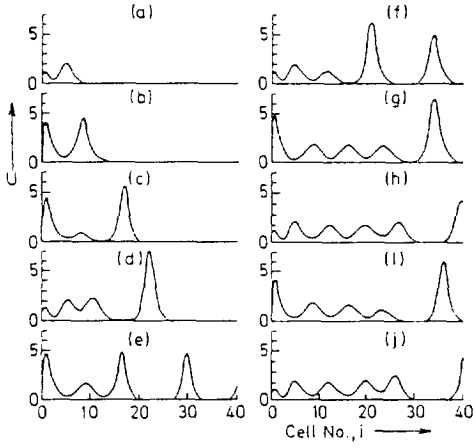

Fig. 16. Spatial concentration profiles in the 1-D cell model.

Da=8.0, $\alpha_1=\alpha_2=\alpha_3=0.2$. $K_m=0.0$. Time is: (a) 5.6, (b) 6.6, (c) 11.0, (d) 12.0, (e) 21.4, (f) 22.4, (g) 31.8, (h) 32.8, (i) 318.4, (j) 328.4.

plex multipeak and eventually chaotic-type oscillations. The transition to an irregular behavior occurs near cell twenty-one, see Fig. 14f. A 3-dimensional plot clearly demonstrates the changing type of the oscillations (see Fig. 15a-15c). Chaotic-type behavior in the rear part of the system is depicted in Fig. 15c. This figure shows a "spiral-type" of chaotic oscillations. The corresponding spatial concentration profiles in the 1-D cell model at different times are shown in Fig. 16.

The dynamics of the 1-D cell model can be viewed in terms of a set of forced oscillators. The output concentration from the preceding cell becomes the forcing function of the concentration fed to the next oscillator. When any of these oscillators is subjected to an oscillatory input, synchronization phenomena can be expected. When the frequency of the input is fairly close to the natural frequency, a simple type of forced oscillation occurs. The range implied by "fairly close" depends on the amplitude of the input. The numerical study by Tomita and Kai [25] indicated that at input frequencies near twice the natural frequency, and for sufficiently large input amplitude, the subharmonic oscillation becomes unstable and may give rise to irregular behavior. Fujisaka [26] also showed that a set of two or three coupled oscillators in a discrete model may exhibit chaotic behavior for a certain interval of parameters. Marek and Schreiber [27] also numerically observed chaotic behavior for two identical oscillators of a Brusselator model with different diffusion

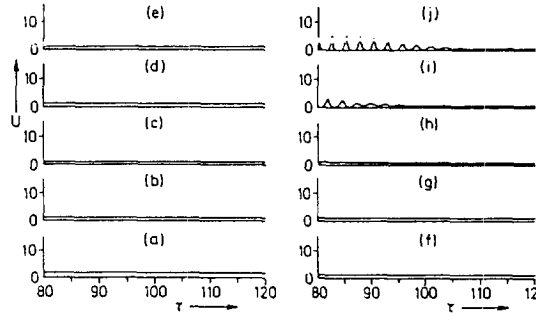

Fig. 17. Temporal behavior at different positions in the 1-D dispersion model.

Da=8.0, $\alpha_1=\alpha_2=\alpha_3=0.2$. Pe=2.09 (Re=100). Axial coordinate is: (a) 1.0, (b) 5.0, (c) 9.0, (d) 13.0, (e) 17.0, (f) 21.0, (g) 25.0, (h) 29.0, (i) 33.0, (j) 37.0.

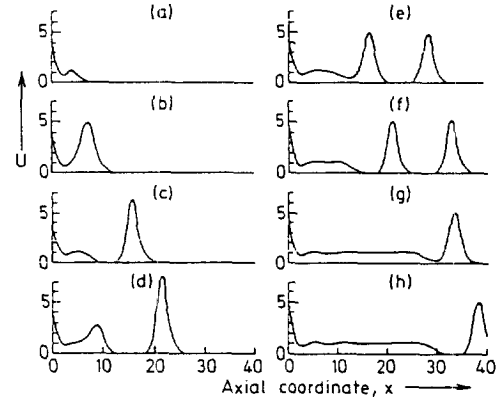

Fig. 18. Spatial concentration profiles in the 1-D dispersion model.

Da=8.0, $\alpha_1=\alpha_2=\alpha_3=0.2$. Pe=2.09 (Re=100). Time is: (a) 5.6, (b) 6.6, (c) 11.0, (d) 12.0, (e) 21.4, (f) 22.4, (g) 71.6, (h) 72.6.

coupling for the two components. Fig. 14 may be said to indicate subharmonic temporal and spatial bifurcations in the tubular system. In a 1-D cell model, the backflow has no significant qualitative effect on the dynamics of oscillatory waves propagating in the reactor. However, an increasing backflow does give rise to a phase lag between the oscillations. This lag increases with time. The backflow rate for mass (K_m) is calculated by using the formula proposed in [28].

The dynamic behavior of the 1-D dispersion model is shown in Fig. 17. The corresponding cell model was displayed in Fig. 14. For low values of the particle-related Peclet number, the temporal behavior of the

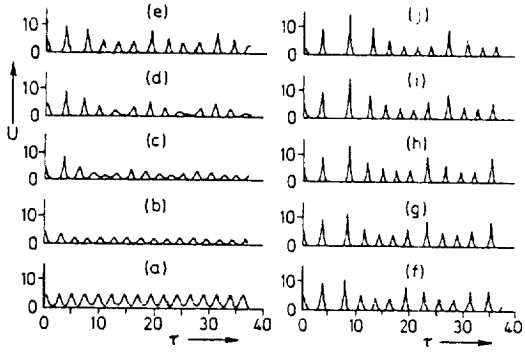

Fig. 19. Temporal behavior at different positions in the 1-D dispersion model.
Da=8.0, $\alpha_1=\alpha_2=\alpha_3=0.2$. Pe=0.72 (Re=0.3). Axial coordinate is: (a) 1.0, (b) 5.0, (c) 9.0, (d) 13.0, (e) 17.0, (f) 21.0, (g) 25.0, (h) 29.0, (i) 33.0, (j) 37.0.

dispersion model closely resembles, in the qualitative way, that observed in the cell model (cf. Fig. 19 with Fig. 14).

Increasing values of Pe in the dispersion model suppresses the occurrence of spatial structures. This conclusion is in accordance with previous results for exothermic reactions [29]. A comparison of axial concentration profiles for the cell and the dispersion model show different types of behavior, see Figs. 16 and 18. We observed irregular dynamic behavior for the cell model while regular oscillations were always established for the dispersion model.

CONCLUSIONS

Dissipative structures of autocatalytic reactions was studied both in distributed and lumped parameter flow systems.

In a continuous stirred tank reactor, uniqueness of steady states exists. A linear stability analysis predicts a stable node, a stable focus, and a saddle-focus to be possible in the CSTR. Sustained oscillations around the unstable focus can occur for high values of the Damköhler number. The period of the oscillations increases with increasing flow rates.

In the distributed parameter system, several kinds of wave phenomena such as travelling, standing and complex oscillatory waves were established.

For low values of Da, Da≅0.01-0.05, travelling pseudo-constant pattern waves were detected. The characteristic steady state shows pattern formation in the spatial dimension.

For intermediate values of Da, Da≅0.1-2.0, single or multiple standing waves were obtained. The number of standing waves increases with increasing values of Da. A numerical simulation starting from different initial conditions revealed that unique multiple standing waves occur. The tempporal behavior, at each position in the system, may exhibit the characteristics of retriggering or echo waves, particularly so at Da=2.0.

For high values of Da, oscillating waves in the spatial dimension were observed. The results of simulation in a 1-D cell model show that regular oscillations can occur near the inlet but these oscillations change into irregular ones at a certain axial position. This suggests that subharmonic limit cycle bifurcations, leading to chaotic behavior, are possible. The effect of backflow does not change the quality of dynamical phenomena in the 1-D cell model except for the fact that increasing the backflow rate shifts the phase lag of the oscillation.

Dynamic properties of the 1-D dispersion model are strongly dependent on the values of Peclet number. Higher values of Pe suppress oscillations. Spatial profiles show a train of pulsating waves in the 1-D cell model and a single pulsating or solitary wave in the corresponding dispersion description.

NOMENCLATURE

C : concentration
D : diffusion coefficient
Da : Damköhler number defined by Eq. (6)
d_p : diameter of particle
F, G, H : defined by Eq. (7)
i : cell number
K_m : mass back flow rate defined by Eq. (6)
k_1, k_2, k_3 : reaction rate constants
N : total cell number
Pe : Peclet number defined by Eq. (6)
q : flow rate
q_m : back flow rate
R_1, R_2, R_3 : reaction rates defined by Eq. (1)
Re : Reynolds number
t : time
u : mean velocity of fluid through tubular flow reactor
U : dimensionless concentration of C_1 defined by Eq. (6)
v : volume of a CSTR
V : dimensionless concentration of C_2 defined by Eq. (6)
W : dimensionless concentration of C_2 defined by Eq. (6)

x : dimensionless axial length defined by Eq. (6)
z : axial length

Greek Letters

α : defined by Eq. (9)
$\alpha, \alpha_2, \alpha_3$: dimensionless rate constants defined by Eq. (6)
β : defined by Eq. (9)
γ : defined by Eq. (9)
δ : defined by Eq. (11)
Δ : delay time
ε : defined by Eq. (11)
ζ : defined by Eq. (11)
λ : eigenvalues
τ : dimensionless time defined by Eq. (6)

Subscripts

i : cell number
s : steady state
o : initial state
1, 2, 3 : components of 1, 2, and 3, respectively

REFERENCES

1. Lotka, A. J.: Elements of Mathematical Biology, Dover (1956).
2. Nicolis, G. and Prigogine, I.: Self-Organization in Non-equilibrium System, John Wiley, New York (1977).
3. Erneux, T. and Herschkowitz-Kaufman, M.: *Bull. Math. Biol.*, **41**, 21 (1979).
4. Herschkowitz-Kaufman, M.: *Bull. Math. Biol.*, **37**, 589 (1975).
5. Prigogine, I. and Lefever, R.: *J. Chem. Phys.*, **48**, 1695 (1968).
6. Vavilin, V. A. and Zhabotinskii, A. M.: *Kinetics and Catalysis*, **10**, 538 (1969).
7. Zhabotinskii, A. M. and Zaikin, A. N.: *Kinetics and Catalysis*, **12**, 516 (1971).
8. Frank-Kamanetskii, D. A.: Diffusion and Heat Transfer in Chemical Kinetics, Plenum Press, New York (1969).
9. Yamazaki, I., Nakamura, S. and Yokota, K.: *Nature*, **222**, 794 (1969).
10. Tatterson, D. F. and Hudson, J. L.: *Chem. Eng. Commun.*, **1**, 3 (1973).
11. Zhabotinskii, A. M. and Zaikin, A. N.: *J. Theor. Biol.*, **40**, 45 (1973).
12. Marek, M. and Svobodova: *Biophys. Chem.*, **3**, 263 (1975).
13. Graziani, K. R., Hudson, J. L. and Schmitz, R. A.: *Chem. Eng. J.*, **12**, 9 (1976).
14. Schmitz, R. A., Graziani, K. R. and Hudson, J. L.: *Chem. Phys.*, **67**, 3040 (1977).
15. Rössler, O. E.: *Nature*, **271**, 89 (1978).
16. Simoyi, R. H., Roux, J. C. and Swinney, H. L.: *Physica*, **8D**, 257 (1983).
17. Roux, J. C.: *Physica*, **7D**, 57 (1983).
18. Hlavacek, V., Sinkule, J. and Kubicek, M.: *J. Theor. Biol.*, **36**, 283 (1972).
19. Sinkule, J., Hlavacek, V., Vortruba, J. and Tvrdik, I.: *Chem. Eng. Sci.*, **29**, 689 (1974).
20. Puszynski, J., Snita, D., Hlavacek, V. and Hofmann, H.: *Chem. Eng. Sci.*, **36**, 1605 (1981).
21. Gray, P. and Scott, S. K.: *Chem. Eng. Sci.*, **38**, 29 (1983).
22. Pisman, L. M.: *Chem. Eng. Sci.*, **38**, 1950 (1980).
23. Neu, J. C.: *SIAM J. Appl. Math.*, **36**, 509 (1979).
24. Krinsky, V. I.: *Science Publ.*, **20**, 59 (1968) (in Russian).
25. Tomita, K. and Kai, T.: *Prog. Theor. Phys.*, **61**, 54 (1979).
26. Fujisaka, H.: *Phys. Lett.*, **A66**, 450 (1978).
27. Marek, M. and Schreiber, I.: *Physica*, **5D**, 258 (1982).
28. Kim, S. H. and Hlavacek, V.: On the Dynamics of Parabolic Equations Describing Diffusion, Convection and a Chemical Reaction, *Physica*, **10D**, 413 (1984).
29. Wen, C. Y. and Fan, L. T.: Models for Flow Systems and Chemical Reactors, Marcel Dekker, Inc., New York (1975).